Published in final edited form as:
Int J Hyperthermia. 2008 November ; 24(7): 537–549. doi:10.1080/02656730802064621.

In vitro and *in vivo* evaluations of increased effective beam width for heat deposition using a split focus high intensity ultrasound (HIFU) transducer

Pretesh R. Patel, **Alfred Luk**, **Amirk Durrani**, **Sergio Dromi**, **Julian Cuesta**, **Mary Angstadt**, **Matthew R. Dreher**, **Bradford J. Wood**, and **Victor Frenkel**
Diagnostic Radiology Department, Clinical Center, National Institutes of Health, Bethesda, MD, USA

Abstract

Purpose—To develop a novel and efficient, *in vitro* method for characterizing temporal and spatial heat generation of focused ultrasound exposures, and evaluate this method to compare a split focus and conventional single focus high intensity focused ultrasound transducer.

Materials and methods—A HIFU tissue-mimicking phantom was validated by comparing respective temperature elevations generated in the phantoms and in murine tumors *in vivo*. The phantom was then used in combination with IR thermography to spatially and temporally characterize differences in low-level temperature elevation (e.g. 3–5°C) produced by a single focus and split focus HIFU transducer, where the latter produces four simultaneous foci. *In vivo* experiments with heat sensitive liposomes containing doxorubicin were then carried out to determine if the larger beam width of the split focus transducer, compared to the single focus, could increase overall deployment of the drug from the liposome

Results—Temperature elevations generated in the HIFU phantom were not found to be different from those measured *in vivo* when compensating for disparities in attenuation coefficient and specific heat, and between the two transducers by increasing the energy deposition. Exposures with the split focus transducer provided significant increases in the area treated compared to the single focus, which then translated to significant increases in drug deposition *in vivo*.

Conclusions—Preliminary evidence was provided indicating the potential for using this novel technique for characterizing hyperthermia produced by focused ultrasound devices. Further development will be required for its suitability for correlating *in vitro* and *in vivo* outcomes.

Keywords

High intensity focused ultrasound; image guided therapy; single focus and split focus transducer; low temperature sensitive liposomes; infrared imaging

Correspondence: Victor Frenkel, PhD, Diagnostic Radiology Department, Clinical Center, National Institutes of Health, Building 10, Room 1N306a, 10 Center Drive, Bethesda, MD 20892, USA. Tel: 301-402-5710. Fax: 301-496-9933. E-mail: vfrenkel@cc.nih.gov.

Declaration of interest: The authors report no conflicts of interest. The authors alone are responsible for the content and writing of the article

Introduction

High-intensity focused ultrasound (HIFU) can be used to non-invasively deposit energy in a relatively small focal zone, compared to other hyperthermia devices (e.g. microwaves), at a distance remote from the transducer, using various modalities of image guidance. Focused ultrasound can deposit energy and produce clinically relevant bio-effects in the targeted tissue, and has been used in a variety of clinical and pre-clinical disease models. Continuous wave HIFU exposures (in the order of seconds) have been used to ablate tissues such as prostate cancer, breast cancer, liver cancer, and uterine fibroids [1]. Heat generation can be significantly reduced to sub-cytotoxic levels with pulsed HIFU exposures, where relatively short duty cycles (in the order of 5–10%) allow non-thermal mechanisms to predominate, such as acoustic cavitation and radiation forces [2]. These exposures have been shown to increase the delivery and consequent therapeutic effects of small molecules, liposomes, and plasmid DNA [2].

Recent advances in chemical engineering have given rise to a new generation of temperature sensitive macromolecular drug carriers that can be paired with external heating sources such as HIFU. Targeted delivery of drug is achieved by the use of thermosensitive drug carriers, improving drug toxicity profiles and increasing the effective dose delivered to targeted tissues. Thermosensitive liposomes (TSLS) are normally stable at physiological temperatures but undergo predictable phase changes when heated, which releases their drug payloads [3]. By providing HIFU exposures in pulsed mode, temporal averaged intensities normally sufficient for ablating tissue are lowered and heat generation can be reduced below levels for tissue destruction [4]. Dromi et al. [5] were able to use pulsed HIFU with relative low duty cycles as a controlled source of image-guided, low-level hyperthermia (39–41°C) that caused deployment of drug payload from low temperature sensitive liposome (LTSL) to improve tumor regression.

As the number of continuous (and pulsed) HIFU applications grows, technical barriers must be addressed regarding the time requirements for safe and effective large volume treatment. Prolonged treatment times require patient immobility and sedation that can reduce the appeal of such procedures and adversely affect their widespread adoption. Many strategies have been employed to minimize treatment times including the use of phased array transducers for more efficient treatment [6], and by increasing the effective volume of treatment of individual exposures by modifying exposure parameters (such as increasing pulse duration) [7], or by using split focus HIFU transducers [8]. In simulation studies by Fan and Hynynen, minimizing the number of ultrasound pulses required to cover the targeted tissue volume was the most important factor in determining treatment time [9]. Both multi-element phased arrays and split focus transducers create broader focal zones, effectively reducing the required number of individual ultrasound exposures required for treatment. Sasaki et al. showed greater focal volumes and reduced treatment times using split focus transducers in swine liver [10].

In this study, we compared a custom built split focus transducer with a larger effective beam width to the conventional single focus transducer previously used by our group. We first validated a previously described gel phantom, employing an exposure correction factor to account for discrepancies in attenuation and specific heat between the phantom and soft tissues. We then introduced a high through-put technique for visualizing spatial heat dynamics, to compare single and split focus exposures, where a large number of samples could be treated quickly and uniformly. Finally, increased spatial heat generation with the split focus transducer was demonstrated by systemic delivery of doxorubicin-loaded LTSLs in combination with HIFU exposure in the limb muscle of mice *in vivo*, followed by extraction and quantification of the drug released in the target tissue.

Materials and methods

Cylindrical and planar gel phantoms

Gel phantoms were prepared according to Lafon et al. [11]. In short, a 40% stock solution of polyacrylamide Liqui-gel 19 : 1 (MP Biomedicals Inc., Irvine, CA) was diluted to 7% by volume with distilled, degassed water. Bovine Serum Albumin (BSA) was added at 7% by weight as a temperature sensitive protein. Polymerization of the gels was achieved by adding N',N'-tetramethylenediamine (0.01 ml/15 ml Liqui-gel) and ammonium persulfate (0.05 ml 10% persulfate/15 ml Liqui-gel).

Cylindrical phantoms were made to simulate the shape of the mice. The final gel composition was poured into 50 ml plastic centrifuge tubes with conical bottoms (VWR, West Chester, PA) and allowed to set. The cylindrical form was thought to best mimic the body of a mouse possessing subcutaneous tumors. Relatively thin, planar phantoms were used to enable measurement of the HIFU induced temperature elevations using an infrared camera. 265 ml of the gel was poured into a rectangular plastic container (14.50 cm×18.25 cm×3.25 cm). The resulting gelled sheets were removed from the container and cut into four sections of equal size (7.25 cm×9.13 cm×1 cm thick). In all cases, the gel phantoms were kept overnight at 4° C and used the next day.

Despite the suitability of gel phantom acoustic properties (e.g. speed of sound and density), a correction factor (CF) for the HIFU exposure parameters was calculated based on the disparities in the phantom's other relevant properties. Since the attenuation coefficient was lower than that of soft tissue and the specific heat was greater, the energy of the exposures was increased in order to generate comparable temperature elevations to soft tissues. A correction factor of 4 was determined (see Appendix) meaning that either the power would have to be increased 4-fold (with the pulse duration constant), the pulse duration increased 4-fold (with the power constant), or any possible combination of the two.

HIFU system

A custom built HIFU system was used for our study, modified from a Sonoblate® 500 (Focus Surgery; Indianapolis, IN), allowing it to operate at a frequency of 1MHz (instead of 4MHz) and enabling various duty cycles to be used (instead of operating only in continuous wave mode). Both probes (single focus and split focus) possessed a therapeutic (1MHz) transducer and a co-axial (10 MHz) imaging transducer, each with a focal length of 4 cm. The concave, spherical therapeutic transducer had a diameter of 5 cm; the imaging transducer's aperture was 0.8 cm. The therapeutic transducer had a maximum available acoustic power of 120W. The focal zone of the single focus transducer was ellipsoid in shape, with an axial length (−3 dB) of 7.2mm and a radial diameter (−3 dB) of 1.38 mm. The split focus transducer was identical to the single focus in all respects with the exception of the focal zone. Simulation studies predict a focal zone with four individual foci theoretically increasing the focal area by a factor of five from 1.49mm^2 (single focus) to 7.4mm^2 (split focus). The focal area was split into four by sectioning the back electrode of the transducer into four equal-area sectors, and driving adjacent sections 180° out of phase [12]. All exposures were carried out using a pulse repetition frequency of 1 Hz. The total acoustic power (TAP) was varied from 20 to 80W, and a duty cycle from 10 (100 ms ON; 900 ms OFF) to 50% (500 ms ON; 500 ms OFF). 120 pulses were given for all exposures, meaning that each total exposure lasted 120 s. The TAP of the transducer was calibrated using the radiation force technique (Lewin et al., 2003).

HIFU exposures

Exposures to compare the tissue-mimicking phantoms with the murine tumor model were carried out in a tank of degassed water at 37°C. A phantom (or mouse) was placed vertically

in a custom built restraint, and connected to a 3D stage (step size = 0.5 mm), which allowed the exposure target to be positioned directly within the focal zone. This same procedure was used for the exposures in the muscle of mice in combination with the LTSLs. For all exposures in the mice, the animals were anesthetized as previously described [4,14].

The planar phantom was used with a membrane-coupled device previously described by Stone et al. [15]. The water-bath was maintained at a temperature of 37°C and the flat phantom temperature was allowed to equilibrate prior to the start of the HIFU exposure.

Real-time temperature measurements

For experiments using the water coupled device, a 4-channel Luxtron Fluoroptic 3100 Series Thermometer (Luxtron Corporation, Santa Clara, CA) was used to monitor temperature elevations for exposures in the submersed cylindrical phantoms and mouse tumors, as previously described by us [4]. One thermocouple was placed in the water-bath, a second was placed in a region of the phantom or tumor well outside of the focal zone, and a third was placed perpendicular to the axial dimension of the focal zone directly adjacent to it using the imaging transducer of the HIFU system. A 22G angiocatheter was employed for inserting and positioning the thermocouples in the mouse tumors [16]. The thermocouples were calibrated in the water-bath using a standard mercury thermometer. Typical data collection started 30 seconds prior to the start of an exposure, and continued for approximately 60 seconds after the temperatures returned to pre-exposure levels. Throughout the exposures, data was acquired from all three thermocouples at 0.25 second intervals. Location of the thermocouple, calibration, and temperature measurements were based on the procedure of Hynynen et al. [16]. The use of the thermocouples in the phantoms and tumor is seen in Figure 1.

A ThermaCAM™ S60 infrared (IR) camera (FLIR Systems, Portland, OR) was used for thermo-graphic monitoring of the surface temperature changes of the planar phantoms during HIFU exposures with the membrane-coupled device. The ThermaCAM™ S60 has a thermal sensitivity of 0.08°C and an accuracy of ±2%. The camera was secured on a tripod and aimed downward at the face of the phantom (Figure 2). The infrared camera recording speed was set at 3Hz (3 frames captured per second). IR data collection began 10 seconds prior to the start of each exposure and continued until the phantom temperatures reached thermal equilibrium. The IR camera captures a surface contour temperature profile as a thermal image for the entire upper surface of the planar phantom at each sample time point.

Using ThermaCam Researcher Pro 2.8, an IR image analysis package, temporal elevations in temperature averaged over two concentric areas were recorded. Isotherms were then set at 3° and 5°C elevation over baseline for each exposure. Images were recorded every 5 seconds and the number of pixels contained in the isothermal region recorded. Thermal dose delivered was calculated for each exposure, at each temperature, and the pooled results are presented as means.

Low temperature sensitive liposomes

Low temperature heat sensitive liposomes (LTSLs) containing doxorubicin were produced as previously described [5], and injected intravenously through the tail vein at a volume of 100 μL and dose of 5 mg/kg immediately prior to the pulsed-HIFU exposures. LTSLs have been previously characterized and deploy drug cargos at temperatures between 39° and 41°C [3].

Animal and tissue models

A subcutaneous, murine squamous cell carcinoma line (SCC7) was used for *in vivo* studies of HIFU exposures in tumors. The cells were cultured in RPMI 1640 medium (Biofluids, Gaithersburg, MD) with 10% fetal calf serum, 2mmL-glutamine, and penicillin-streptomycin

(50 IU ml^{-1} and 50 $\mu g ml^{-1}$), at 37°C with 5% CO_2. The cells were pre-tested as my-coplasm-negative (Research Animal Diagnostic Laboratory, University of Missouri, MO).

All animal work was performed according to an approved animal protocol and in compliance with NIH Clinical Center Animal Care and Use Committee guidelines. Female C3H mice were injected with a suspension of SCC7 cells (1×10^6 cells in 100 μL of phosphate buffered saline) in each flank. Tumor volumes were measured every second day using calipers. Tumors received HIFU exposures when reaching a volume of 0.7–0.8 cm^3, which required 7–10 days of growth. For experiments using skeletal muscle, exposures were carried out in the thigh, adjacent to the region where tumors were grown.

Quantitative drug delivery assays

Quantitative assays were carried out as previously described [4,5]. Fluorescence readings were interpolated from values from a standard curve generated by serial dilutions of doxorubicin. In the first of the two LTSL experiments, the total amount of doxorubicin in each sample was determined. In the second experiment, the amount of doxorubicin was normalized by weight. For both experiments, group values were pooled and presented as means.

Experimental exposures

Three separate experiments were carried out as described below. The experimental exposures are summarized in Table I.

Validation of the phantom, I—The object of this first experiment was to validate the phantoms as a suitable tissue-mimicking material. Exposures were given in the tumors and the cylindrical phantoms with the single focus transducer. These exposures carried out in the water-bath and temperature elevations were measured using the fluorometric thermocouples. For exposures in the phantoms, the power was increased 4-fold (from 20W to 80W), as predicted by the correction factor (calculated above) for the phantoms.

Comparison of single and split focus, II—The objective of this second experiment was to compare the overall region of treatment between the single focus and split focus transducers. The planar phantoms were used for these experiments, where exposures were carried out with the membrane-coupled device. Temperature elevations were measured using the IR camera. A 20W exposure was used for the single focus transducer, and an 80W exposure used with the split focus. Preliminary experiments with the single focus showed that the duty cycle needed to be increased from 10% to 50% in order to obtain temperature elevations comparable to those obtained in the cylindrical phantoms in the water-bath (at 80W, with a duty cycle of 10%).

Validation of split focus*in vivo*, III—Exposures were carried out in the muscle of mice using both the single focus and split focus transducers, with the system in a water-bath. The LTSLs were injected intravenously into mice immediately prior to HIFU exposures. Two exposures were compared: a single exposure with the single focus transducer and a single exposure with the split focus transducer. Immediately after the exposures the animals were euthanized and the exposed tissue was analysed for doxorubicin concentration. Two additional drug-only control groups were used without HIFU exposures. In one, LTSLs were administered; in the second, free doxorubicin without delivery liposome.

Statistical analysis

Analysis of the data was carried out using the JMP (SAS Institute, Cary, NC) software package. A regression analysis was used for determining the relationship between duty cycle and mean temperature elevation in the cylindrical phantoms. *T*-tests were used to compare mean temperature elevations of the cylindrical phantoms and the tumors, the mean area under the

curve (AUC) for isotherm temperature elevations in planar phantoms, and the mean concentration doxorubicin in the control LTSL experiment. A Tukey-Kramer HSD test was used to compare all pair combinations of the group means of total doxorubicin content in the HIFU LTSL experiment. A *P* value of less than 0.05 was considered statistically significant.

Results

Gel phantom validation results

A comparison of HIFU exposures showed that mean temperature elevations in the cylindrical phantom (when using the correction factor) were not significantly different compared to tumors (both at a duty cycle of 10%). Exposure without the correction factor in the cylindrical phantoms produced far lower temperature elevations, such that they could not consistently be detected (Figure 3a). HIFU exposures in the cylindrical phantom produced average steady state temperature elevations of 4.2° ±0.54°, 12.2° ±4.98°, 17.3° ±6.52° and 23.7° ±5.85°C for duty cycles of 10, 20, 30 and 40%, respectively. Figure 3(b) shows that a linear relationship exists between duty cycle and the temperature increase in the phantom, where the following linear equation describes the data:

$$\Delta T[^{\circ}\mathrm{C}]=0.61*\mathrm{DC}[\%]-0.603,$$

where DC = duty cycle (R^2 = 0:9935; P = 0:0002)

Single to split focus comparisons in planar gel phantoms

Temperature elevation to threshold values of 3°C and 5°C in planar phantoms following HIFU exposures with both single focus and split focus devices are presented in Figure 4. Temperature elevations for split focus exposures at power input levels below 80W were lower than the single focus transducer (data not shown). Temperature elevations, modeled by linear regression, were used to calculate area under the curve (AUC). These results are summarized in Table II.

AUC was increased 3.2 and 2.8-fold when using the split focus transducer to produce temperature elevations of at least 3° and 5°C, respectively (Table II, Figure 5).Figure 6 depicts a representative set of images that characterize the heating signature of the single focus and split focus transducers from the start of treatment, 0s, to the end, 120s. Multiple foci of temperature elevation are present in the split focus IR images but absent for the single focus.

In vivo results

Exposures with the split focus transducer at 80W yielded 1.650 μg of total doxorubicin while the single focus transducer at 20W yielded 0.834 μg, a 1.98-fold difference (*P* = 0.02). Internal controls from both groups showed a 1.95-fold increase (*P* = 0.04) with the split focus transducer (0.659 μg) compared to the single focus transducer (0.338 μg). The results are summarized in Figure 7(a). Control experiments with no HIFU exposure yielded 2.90 μg/g for free doxorubicin versus 0.726 μg/g for LTSL (*P* = 0.001) (Figure 7b).

Discussion

The ability to tightly focus ultrasound energy into a small volume has led to a number of emerging therapeutic ultrasound applications including thermal ablation, hemorrhage control and drug delivery. Using image guidance to deposit energy in well defined target tissue enhances safety and accuracy. Such tightly focused energy can require a great number of exposures and time to treat a large target volume. This increases treatment time and impairs clinical adoption and could add to potential morbidity. Hence, increasing the volume of the

focal region can reduce the duration of a particular treatment, where the reduction in time should be proportional to the increase in volume of the individual exposures.

Technical modifications have been evaluated in a variety of ablation technologies to increase the through-put of energy deposition. Multi-probe radio-frequency ablation [17], multi-antennae microwave ablation [18], multiple fiber laser-induced thermotherapy (LITT) [19], and split focus HIFU [8] all aim to reduce treatment times without compromising efficacy and safety. By sectioning the back electrode of the HIFU transducer and driving adjacent sections 180° out of phase, the focal region of the beam can be split into four without significant elevations in peak intensities in front and behind the focal zone [12]. In this way the split focus transducer can increase the spatial through-put of energy deposition while retaining the safety profile of single focus transducers.

Systematic comparison of novel split focus devices will allow quicker translation of promising technologies to the clinic. Simulation studies are commonly used to evaluate new transducer designs prior to fabrication. Sasaki et al., for example, used a 3-D thermal model, to evaluate a number of split focus transducers, each possessing a separate design [10]. In this study, we employed tissue mimicking phantoms and non-invasive infrared imaging as a novel analysis methodology to evaluate split focus HIFU transducers. Tissue-mimicking phantoms are often employed to first evaluate the heating potential of new medical devices before they are used with human patients [20]. Substituting phantoms for live animal tissue has many advantages, including less cost, fewer animal requirements, less labor-intensive experimentation, and more dependable and predictable results.

Ultrasound phantoms have been developed with a variety of compositions, which include agar [21], gelatin [22], polyvinyl alcohol [23], polyacrylamide [24], and acrylamide cross-linked with bis-acrylamide [25]. In the latter two phantoms, bovine serum albumin (BSA) can be added, in order to indicate a localized response to the heating by high intensity focused ultrasound (HIFU). The resulting lesions, formed by the denaturation of the protein, are then visible to the naked eye, being opaque in the otherwise transparent phantoms. The lesions, which become hyperechoic, may also be imaged using ultrasound B-mode imaging [24], magnetic resonance imaging (MRI) [25], and computed tomography (CT) [26]. These acrylamide phantoms, also known as hydrogels, are hydrophilic gels composed of cross-linked polymer networks saturated with water. The gel phantoms are easy to make, and because they possess mechanical properties similar to those of water, they can be created into rigid 3-dimensional shapes [27] suitable for different conditions of HIFU exposure. Phantoms for HIFU are becoming a necessary tool for everyday performance testing and calibration in therapeutic ultrasound laboratories [24].

There are a number of limitations for using phantoms to mimic live animal tissue, such as the absence of circulatory perfusion (which can affect heat transfer in response to local energy deposition) and a deviation of some of their physical properties from those of live tissue. However, phantoms can be extremely useful as an alternative to using live animals, as long as their limitations are taken into account in the interpretations of the experimental results.

As reported by Prokop et al. [27], polyacrylamide gel phantoms are easy to fabricate into custom shapes that closely represent the shapes of various solid tissue. The cylindrical shaped phantom used in this study with the water-coupled device was a good model for a submerged mouse with tumor. This system has been used for exposing various subcutaneously grown tumors in the flanks of mice [4,5,14,28]. In this system, both the transducer and the mice were held in an upright position across from each other at a distance equal to that of the transducer's focal zone. Both the cylindrical phantom and the subcutaneous mouse tumors allowed for easy insertion of thermocouples for temperature measurements.

The phantom selected for this study possessed a similar density and speed of sound to that of the liver, a typical soft tissue often used for *ex vivo* HIFU studies [29]. This meant that its impedance would be similar, and in that way would minimize the amount of energy reflected at the water-phantom interface. However, the attenuation coefficient of the phantom was lower than that of the liver and the specific heat capacity was higher. The consequence of each of these disparities alone would be that temperature elevations in the phantoms with a particular exposure would be less than those found *in vivo* using the same exposure. In Lafon et al. [24] for example, where attenuation coefficients of their hydrogels were considerably lower (≈8 fold), significantly lower lesion volumes were observed compared to those in *ex vivo* turkey breast tissue with the same HIFU dose (J cm^{-2}). In the present study, the lower attenuation coefficient and the higher specific heat of the phantoms (compared to the tissue) resulted in temperature elevations that were so low (compared to the tissue) that they could not consistently be detected.

In the present study, incorporating the ratios (i.e. phantom/liver) of the attenuation coefficient and the specific heat capacity in a bioheat equation predicted that these differences could effectively be cancelled out by simply increasing the total acoustic energy applied by a (correction) factor of 4. Indeed, in the first part of the study, when the power was increased 4-fold for exposures in the cylindrical phantoms in the water-coupled system (where all other exposure parameters were kept the same as in the tumors), the differences in mean temperature elevation measured were not found to be statistically significant. These temperature elevations were also approximately the same as previously found with the same exposures in a different tumor model [4]. When using the planar phantoms with the membrane-coupled system, preliminary experiments showed that increasing the duration of the pulses 5-fold produced similar temperature elevations to those in the tumors and cylindrical phantoms. The fact that a correction factor of 5 was needed for these exposures and not 4 could be explained by additional heat losses due to the experimental set-up such as loss of heat at the interface [30] and phantom exposure to ambient temperature. In these experiments with the planar phantoms, where comparisons were carried out between the single and split focus transducers, the pulse duration was increased, and not the power, seeing that a 4-fold increase in power was required for the split focus transducer to produce comparable spatial averaged temperature elevations to the single focus.

The use of planar phantoms in combination with a membrane-coupled system allowed us to be able to non-invasively monitor temperature by infrared (IR) thermography. Thermography is a diagnostic technique where IR imaging is used to measure temperature variations on the surface of the body. Thermography has been shown to be useful as a non-invasive imaging modality, especially in the fields of dermatology, rheumatology, orthopedics, and circulatory abnormalities [31]. It has also been used to investigate phenomena related to ultrasound-induced hyperthermia *in vivo* [32], and in tissue mimicking phantoms with both ultrasonic [32] and non-ultrasonic [22,33] hyperthermia devices.

Using IR thermography, device-dependent heating patterns were observed in planar phantoms treated by both single focus and split focus transducers using a membrane-coupled system. For temperature elevations of at least 3° and 5°C, the split focus transducer produced spatial increases of approximately 3-fold in regard to the radial distribution, indicating that the effective beam width for heat deposition was significantly increased. According to theoretical modeling [12], measurements taken with hydrophones [23] or Schlieren imaging [34], and observations in ablated tissue, the split focus transducers produce four distinct focal zones. Temporal analysis in this study with the phantoms enabled actual visualization of the process by which each of the foci in the split produces an individual temperature increase that over time meld into each other to create one larger hot region.

Comparison of heat deposition between the single focus and split focus transducers was carried out at a temperature increase of 3° and 5°C, corresponding to the threshold temperature and ideal temperature for releasing doxorubicin encapsulated in LTSLs [5]. The area treated above this threshold value was approximately 3-fold greater for exposures using the split focus transducer when power input was corrected at 4-fold, compared to the single focus device. Heat loss due to the experimental set-up may explain why the theoretical 4-fold increase was not observed. The membrane-coupled system introduces additional acoustic boundaries where energy losses may occur: (1) water-bath, (2) water/membrane interface, (3) membrane/phantom interface, and (4) conductive loss from the air-exposed phantom surface.

In the final stage of the study, we hypothesized that the spatial increase in temperature elevation observed with the split focus device could be used to decrease treatment time for release of doxorubicin from LTSLs *in vivo* by decreasing the number of raster (i.e. treatment) points required for treatment. Temperature elevations of 5°C (to 42°C *in vivo*) increase the amount of drug released approaching 100% with prolonged hyperthermia [3]. Dromi et al. successfully triggered release of doxorubicin from LTSLs using the same conventional single focus transducer examined in the present study [5]. Comparing at a single raster point, the split focus transducer, with power compensation, increased the release of doxorubicin from LTSLs by a factor of 1.98 when compared to the single focus transducer. Increased drug deposition in tissue did not scale with increased area of temperature elevation in the phantoms, 2-fold versus 3-fold, respectively. That the 3-fold advantage was not realized could be due a number of reasons. Isotherm area measurements in the tissue phantom experiments set hard cut-off values of 3° and 5°C. However, the liposomes undergo a phase change and begin releasing doxorubicin between 39° and 40°C, or 2°–3°C elevation from baseline [35]. These lower elevations in temperature, occurring at the periphery of the treatment zone, constitute a relatively larger area in the single focus heating signatures. This means that relatively greater amounts of deployment would have occurred with the single focus device than predicted with the phantom experiments, decreasing the difference between the two devices. Although peak temperature elevations for the single focus transducer had previously been measured to be optimal for triggering LTSLs for doxorubicin deployment [4], potentially higher temperature elevations in the geometrical center of the split focus transducer may not have been optimal. The permeability of thermo-sensitive liposomes rapidly increases at the threshold temperature and then starts to drop off at higher temperatures [36]. This phenomenon would have decreased the consequent deployment, and lead to a further overall net reduction with the split focus.

In this experiment, several parameters differed from a clinically relevant treatment protocol. It is important to note that temperature elevations *in vivo* were not specifically tuned to optimize doxorubicin release from LTSLs. This would be a necessary first step in any clinical application of this technology. Treatment at multiple raster points, as in Dromi et al. [5], would certainly be required for treatment of large tumors. Muscle tissue, instead of tumor, was used for its structural uniformity and tight vasculature in order to minimize variance. Hyperthermia is known to preferentially increase the permeability of tumor vasculature compared to normal tissue [37]. Subsequently, the transvascular transport of LTSLs and released doxorubicin is expected to be increased in tumor. By treating with a larger focal zone and reducing total treatment time, fewer cardiac cycles will elapse during treatment with the split focus transducer reducing the exposure of administered liposomes to the reticuloendothelial system. A greater percentage of the dose is then available for deposition in the HIFU exposed tumor effectively increasing the peak dose delivered. Taking into account these types of ancillary benefits, the true advantage of split focus HIFU treatment may be even more meaningful than a 2–3 fold reduction in treatment time as indicated by this study.

Although not part of the originally designed study, the final experiment demonstrated that doxorubicin in free form accumulated in muscle to a 4-fold higher concentration than

doxorubicin contained within the LTSLs at an early time point (5 min). This experiment was carried out to explain why control tissue for the split focus had 2-fold higher levels of doxorubicin than control tissue for the single focus; the same fold increase for the treated tissue with each device. One possible explanation for this increased doxorubicin concentration in the control tissue when using a split focus is that free doxorubicin was deployed from the LTSL within the treated tissue that subsequently accumulated in the control tissue. The extraction fraction (i.e., fraction of solute in the plasma that is extracted by the tissue) of free doxorubicin ranges from 0.13 to 0.24 [38], and we can assume that the extraction fraction of doxorubicin contained within the liposome is far lower as demonstrated by Figure 7(b). More doxorubicin is locally deployed from the LTSL using the split focus (see Figure 7a) such that some free doxorubicin remained in circulation and is therefore available to be taken up in the rest of the body including the control tissue. The significantly higher amount of doxorubicin found in the control tissue using the split focus suggests that a portion of the doxorubicin released in the treated muscle remained in circulation and accumulated to a greater extent in untreated tissues of the body.

In this study we evaluated the use of a combination of thermography and tissue phantoms as a simple, high through-put method to evaluate the heating characteristics of hyperthermia devices, namely HIFU transducers. Allowing for both temporal and spatial monitoring, the evolution of temperature elevation during treatment may be analysed for more rigorous comparison of the heating characteristics of experimental devices. Though not a replacement for *in vivo* experiments, preliminary comparisons between hyperthermia devices may be undertaken using tissue phantoms and IR thermography.

Acknowledgements

Many thanks go to Dr Robert J. Lutz of the National Institutes of Health (Bethesda, MD) for all matters related to thermography, and to Celsion Corp. for providing the materials and technical instruction for producing the LTSLs. We also thank Stephen R. Knight Jr for providing much needed expertise in computer-related issues. The research was supported in part by the intra-mural research program of the Clinical Center, National Institutes of Health, USA.

References

1. Kennedy JE. High-intensity focused ultrasound in the treatment of solid tumours. Nat Rev Cancer 2005;5:321–327. [PubMed: 15776004]
2. Frenkel V, Li KC. Potential role of pulsed-high intensity focused ultrasound in gene therapy. Future Oncol 2006;2:111–119. [PubMed: 16556078]
3. Kong G, Dewhirst MW. Hyperthermia and liposomes. Int J Hyperthermia 1999;15:345–370. [PubMed: 10519688]
4. Frenkel V, Etherington A, Greene M, Quitjano J, Xie J, Hunter F, Dromi S, Li KC. Delivery of liposomal doxorubicin (Doxil) in a breast cancer tumor model: Investigation of potential enhancement by pulsed-high intensity focused ultrasound exposure. Acad Radiol 2006:469–479. [PubMed: 16554227]
5. Dromi S, Frenkel V, Luk A, Traughber B, Angstadt M, Bur M, Poff J, Xie J, Libutti SK, Li KC, et al. Pulsed-high intensity focused ultrasound and low temperature-sensitive liposomes for enhanced targeted drug delivery and antitumor effect. Clin Cancer Res 2007:2722–2727. [PubMed: 17473205]
6. Ebbini ES, Cain CA. A spherical-section ultrasound phased array applicator for deep localized hyperthermia. IEEE Trans Biomed Eng 1991;38:634–643. [PubMed: 1879855]
7. Damianou C, Hynynen K. The effect of various physical parameters on the size and shape of necrosed tissue volume during ultrasound surgery. J Acoust Soc Am 1994;95:1641–1649. [PubMed: 8176064]
8. Cain CA, Umemura S. Concentric-ring and sector-vortex phased-array applicators for ultrasound hyperthermia. IEEE Trans Microwave Theory Tech 1986;34:542–551.
9. Fan X, Hynynen K. Ultrasound surgery using multiple sonications – Treatment time considerations. Ultrasound Med Biol 1996;22:471–482. [PubMed: 8795174]

10. Sasaki K, Azuma T, Kawabata KI, Shimoda M, Kokue EI, Umemura SI. Effect of split-focus approach on producing larger coagulation in swine liver. Ultrasound Med Biol 2003;29:591–599. [PubMed: 12749929]
11. Lafon, C.; Kaczkowski, PJ.; Vaezy, S. Development and characterization of an innovative synthetic tissue-mimicking material for high intensity focused ultrasound (HIFU) exposures. IEEE Ultrasonics Symposium; Atlanta, GA. 2001.
12. Seip, R.; Sangvhi, NT.; Uchida, T.; Umemura, SI. Comparison of split-beam transducer geometries and excitation configurations for transrectal prostate HIFU treatments. IEEE Ultrasonics Symposium; Atlanta, GA. 2001.
13. Lewin PA, Barrie-Smith N, Ide M, Hynynen K, Macdonald M. Interlaboratory acoustic power measurement. J Ultrasound Med 2003;22:207–213. [PubMed: 12562125]
14. Dittmar KM, Xie J, Hunter F, Trimble C, Bur M, Frenkel V, Li KC. Pulsed high-intensity focused ultrasound enhances systemic administration of naked DNA in squamous cell carcinoma model: Initial experience. Radiology 2005;235:541–546. [PubMed: 15798154]
15. Stone MJ, Frenkel V, Dromi S, Thomas P, Lewis RP, Li KC, Horne M 3rd, Wood BJ. Pulsed high-intensity focused ultrasound enhanced tPA mediated thrombolysis in a novel in vivo clot model, a pilot study. Thromb Res 2007;121:193–202. [PubMed: 17481699]
16. Hynynen K. The threshold for thermally significant cavitation in dog's thigh muscle in vivo. Ultrasound Med Biol 1991;17:157–169. [PubMed: 2053212]
17. Goldberg SN, Gazelle GS, Dawson SL, Rittman WJ, Mueller PR, Rosenthal DI. Tissue ablation with radiofrequency using multiprobe arrays. Acad Radiol 1995;2:670–674. [PubMed: 9419623]
18. Wright AS, Lee FT Jr, Mahvi DM. Hepatic microwave ablation with multiple antennae results in synergistically larger zones of coagulation necrosis. Ann Surg Oncol 2003;10:275–283. [PubMed: 12679313]
19. Veenendaal LM, de Jager A, Strapper G, Borel Rinkes IH, van Hillegersberg R. Multiple fiber laser-induced thermo-therapy for ablation of large intrahepatic tumors. Photomed Laser Surg 2006;24:3–9. [PubMed: 16503781]
20. Stauffer PR, Rossetto F, Prakash M, Neuman DG, Lee T. Phantom and animal tissues for modeling the electrical properties of human liver. Int J Hyperthermia 2003;19:89–101. [PubMed: 12519714]
21. Arora D, Cooley D, Perry T, Skliar M, Roemer RB. Direct thermal dose control of constrained focused ultrasound treatments: Phantom and in vivo evaluation. Phys Med Biol 2005;50:1919–1935. [PubMed: 15815104]
22. Bailey CA, Cowan TM, Liu VG, Lemley EC, Chen WR. Optimization of selective hyperthermia. J Biomed Opt 2004;9:648–654. [PubMed: 15189104]
23. Surry KJ, Austin HJ, Fenster A, Peters TM. Poly(vinyl alcohol) cryogel phantoms for use in ultrasound and MR imaging. Phys Med Biol 2004;49:5529–5546. [PubMed: 15724540]
24. Lafon C, Zderic V, Noble ML, Yuen JC, Kaczkowski PJ, Sapozhnikov OA, Chavrier F, Crum LA, Vaezy S. Gel phantom for use in high-intensity focused ultrasound dosimetry. Ultrasound Med Biol 2005;31:1383–1389. [PubMed: 16223642]
25. McDonald M, Lochhead S, Chopra R, Bronskill MJ. Multimodality tissue-mimicking phantom for thermal therapy. Phys Med Biol 2004;49:2767–2778. [PubMed: 15285246]
26. Wood, BJ.; Yanof, J.; Frenkel, V.; Viswanathan, A.; Dromi, S.; Kruecker, J.; Bauer, C.; Li, KCP. Ultrasound guided stereotactic high intensity focused ultrasound (HIFU). 5th International Symposium on Therapeutic Ultrasound; Boston, MA. 2005.
27. Prokop AF, Vaezy S, Noble ML, Kaczkowski PJ, Martin RW, Crum LA. Polyacrylamide gel as an acoustic coupling medium for focused ultrasound therapy. Ultrasound Med Biol 2003;29:1351–1358. [PubMed: 14553813]
28. Yuh EL, Shulman SG, Mehta SA, Xie J, Chen L, Frenkel V, Bednarsk MD, Li KC. Delivery of systemic chemotherapeutic agent to tumors by using focused ultrasound: Study in a murine model. Radiology 2005;234:431–437. [PubMed: 15671000]
29. Makin IR, Mast TD, Faidi W, Runk MM, Barthe PG, Slayton MH. Miniaturized ultrasound arrays for interstitial ablation and imaging. Ultrasound Med Biol 2005;31:1539–1550. [PubMed: 16286031]
30. Haken BA, Frizzell LA, Carstensen EL. Effect of mode conversion on ultrasonic heating at tissue interfaces. J Ultrasound Med 1992;11:393–405. [PubMed: 1495131]

31. Jiang LJ, Ng EY, Yeo AC, Wu S, Pan F, Yau WY, Chen JH. A perspective on medical infrared imaging. J Med Eng Technol 2005;29:257–267. [PubMed: 16287675]
32. Moros EG, Novak P, Straube WL, Kolluri P, Yablonskiy DA, Myerson RJ. Thermal contribution of compact bone to intervening tissue-like media exposed to planar ultrasound. Phys Med Biol 2004;49:869–886. [PubMed: 15104313]
33. Sherar MD, Gladman AS, Davidson SR, Easty AC, Joy ML. Infrared thermographic SAR measurements of interstitial hyperthermia applicators: Errors due to thermal conduction and convection. Int J Hyperthermia 2004;20:539–555. [PubMed: 15277026]
34. Azuma T, Tomozawa A, Umemura S. Observation of ultrasonic wave-fronts by synchronous Schlieren imaging. Jap J Applied Physics 2002;41:3308–3312.
35. Kong G, Anyaramthatla G, Petros WP, Braun RD, Coluin OM, Needham D, Dewhirst MW. Efficacy of liposomes and hyperthermia in a human tumor xenograft model: Importance of triggered drug release. Cancer Res 2000;60:6950–6957. [PubMed: 11156395]
36. Mills JK, Needham D. The materials engineering of temperature-sensitive liposomes. Methods Enzymol 2004;387:82–113. [PubMed: 15172159]
37. Gerlowski LE, Jain RK. Effect of hyperthermia on microvascular permeability to macromolecules in normal and tumor tissues. Int J Microcirc Clin Exp 1985;4:363–372. [PubMed: 4086191]
38. Ballet F, Vrignaud P, Robert J, Rey C, Poupon R. Hepatic extraction, metabolism and biliaryexcretion of doxorubicin in the isolated prefused rat-liver. Cancer Chemo Pharmacol 1987;19:240–245.
39. Divkovic GW, Liebler M, Braun K, Dreyer T, Huber PE, Jenne JW. Thermal properties and changes of acoustic parameters in an egg white phantom during heating and coagulation by high intensity focused ultrasound. Ultrasound Med Biol 2007;33:981–986. [PubMed: 17434665]
40. Nightingale K, Soo MS, Nightingale R, Trahey G. Acoustic radiation force impulse imaging: In vivo demonstration of clinical feasibility. Ultrasound Med Biol 2002;28:227–235. [PubMed: 11937286]

Appendix

Correction factor (CF) for the gel phantoms

Lafon et al. [11] provides the following data for comparing the properties of a typical soft tissue (e.g.liver) with their tissue-mimicking phantom that was used in the present study:

	Liver	Phantom
Density (kgm^{-3})	1065	1044
Speed of sound ($m\ s^{-1}$)	1549	1544
Attenuation ($Np\ cm^{-1}MHz^{-1}$)	0.049	0.009 – 0.021**
Specific heat ($J\ kg^{-1}K^{-1}$)	3600	4270*

* Lafon et al. [24] more recently found this value of specific heat [39] to be more accurate than 5100, as originally presented.

** The attenuation slope for the phantom is given as 0.009 to $0.021 Npcm^{-1}MHz^{-1}$ for a range of BSA concentrations from 3 to 9%. Assuming a linear relationship exists between both factors, the following equation can be used for determining the attenuation at a set BSA concentration:

$$\text{attenuation } (Np\ cm^{-1}\ MHz^{-1} = \frac{0.003\% + [\text{BSA concentration}(\%)]}{500} \quad (1)$$

For a BSA concentration of 7% used in this study, the corresponding attenuation of the phantom would be $0.017 Npcm^{-1}MHz^{-1}$.

Because the phantoms lacked any mechanisms for convective heat loss (i.e. blood perfusion was absent), and since relatively low temperatures were being generated by the exposures (and thermal conduction is driven by the temperature gradient), a simple bioheat transfer equation, without a heat loss component can be used for approximately predicting the increase in temperature as a result of the ultrasound exposures [40]:

$$\Delta T = \frac{2afI}{\rho C} t, \text{ where } I = P/A \tag{2}$$

where: a is the attenuation coefficient of the tissue [$Npcm^{-1}MHz^{-1}$]; f is the operating frequency [MHz]; P is the power ($J\ s^{-1}$); A is the cross sectional area of the focal zone of the HIFU beam); ρ is the density of the tissue [gcm^{-3}]; C is the specific heat of the tissue [$J\ g^{-1}{}^{\circ} C^{-1}$]; t is the pulse duration [s].

The temperature increase predicted by Equation (2) is set to be identical in both the tissue (ti) and the phantom (ph):

$$\frac{2a_{ti} f_{ti} (P_{ti}/A)}{\rho_{ti} C_{ti}} t_{ti} = \frac{2a_{ph} f_{ph} (P_{ph}/A)}{\rho_{ph} C_{ph}} t_{ph} \tag{3}$$

The operating frequency is a constant for the transducers as is the cross-sectional surface area of the focal zone. Regarding the exposure parameters, the pulse repetition frequency and the number of pulses are both kept constant. The remaining two parameters, the power and the pulse duration, determine the energy applied to each pulse:

$$E[J] = P[J/s] \times t[s] \tag{4}$$

The compensating increase in energy to be applied during each pulse for the phantoms in order to obtain the same temperature elevation in the tissue can be expressed by the following correction factor:

$$CF = \frac{P_{ph} t_{ph}}{P_{ti} t_{ti}} = \frac{\rho_{ph} C_{ph}}{a_{ph}} \times \frac{a_{ti}}{\rho_{ti} C_{ti}} \tag{5}$$

Using the corresponding liver tissue and phantom values described above, and the phantom attenuation coefficient determined from equation 1(BSA conc. = 7%), CF = 3.35. (Empirical data from preliminary experiments (not shown), however, indicated that a CF value of approximately 4 was more appropriate.) For experiments carried out in this study, this meant that either the power would have to be increased four-fold (with the pulse duration constant), the pulse duration increased four-fold (with the power constant), or any number of combinations of the two resulting in a CF equal to 4.

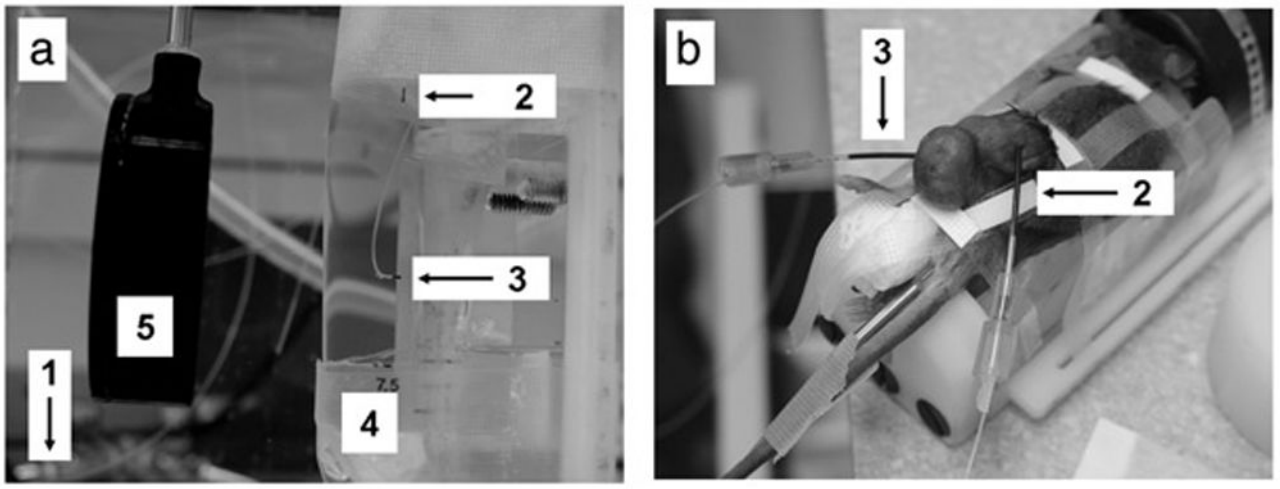

Figure 1.
Water coupled system. (a) Cylindrical phantoms (5) were held in a tank of degassed water at the focal distance of the single focus transducer (4). Temperature of degassed water was monitored (1) and held constant. Temperature elevations were monitored by thermal couples in controls (no exposure) (2) and HIFU exposed phantoms (3). (b) Mice were anesthetized and held in the tank in the same manner as phantoms. Similarly, temperature elevations by thermal couples were monitored in controls (no exposure) (2) and HIFU exposed tumors (3).

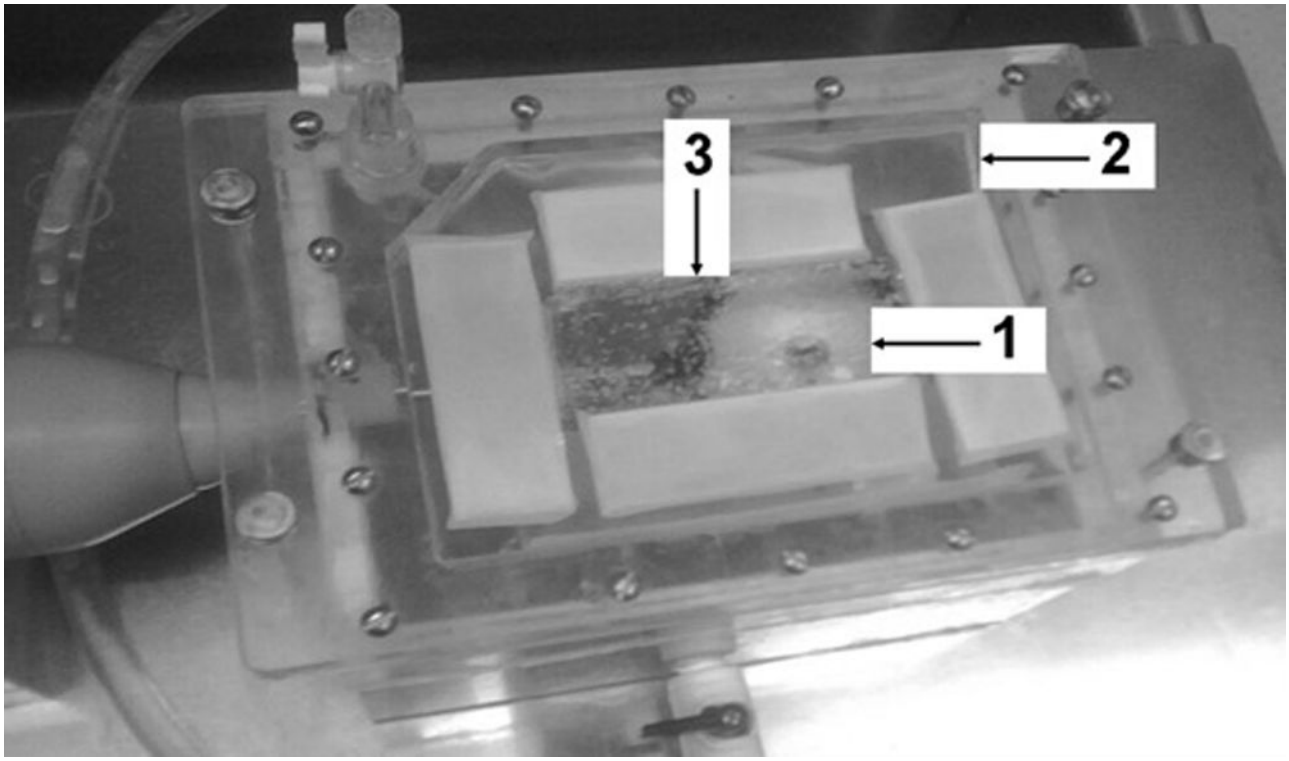

Figure 2.
Membrane coupled system. Both single and split focus transducers were housed in a sealed chamber of degassed water. Planar phantoms (3) were placed on the membrane (2) and held at the focal distance of both transducers (1).

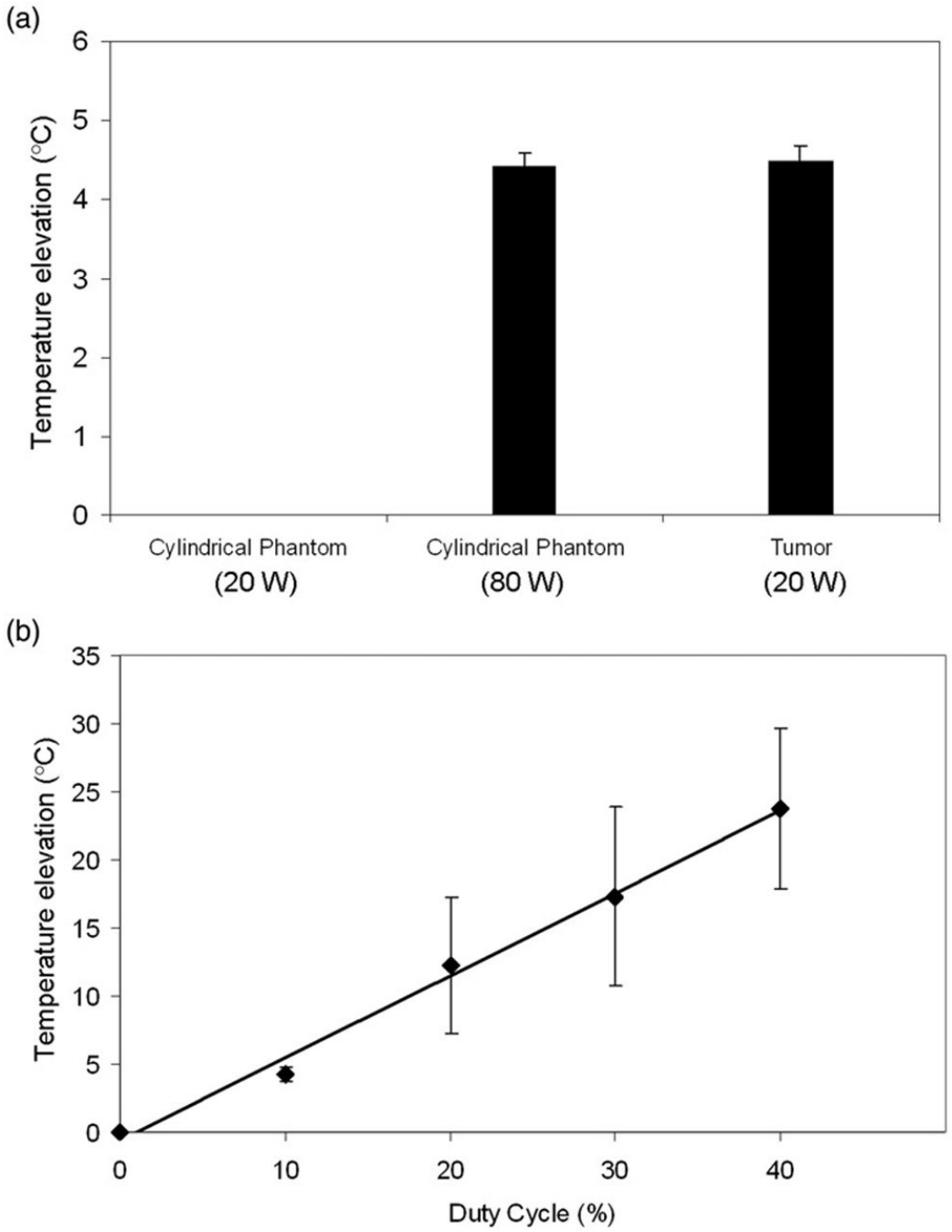

Figure 3.

(a) Temperature elevation in cylindrical phantoms at 80W compared to tumor tissue at 20W. A significant difference was not found between the two. At 20W, temperature elevations in the phantoms were not sufficiently high to be determined accurately. Columns, mean (n = 5); bars, standard deviation. (b) Linear relationship between duty cycle (%) and peak temperature elevation in cylindrical phantoms (80W). Points, mean (n = 5); bars, standard deviation.

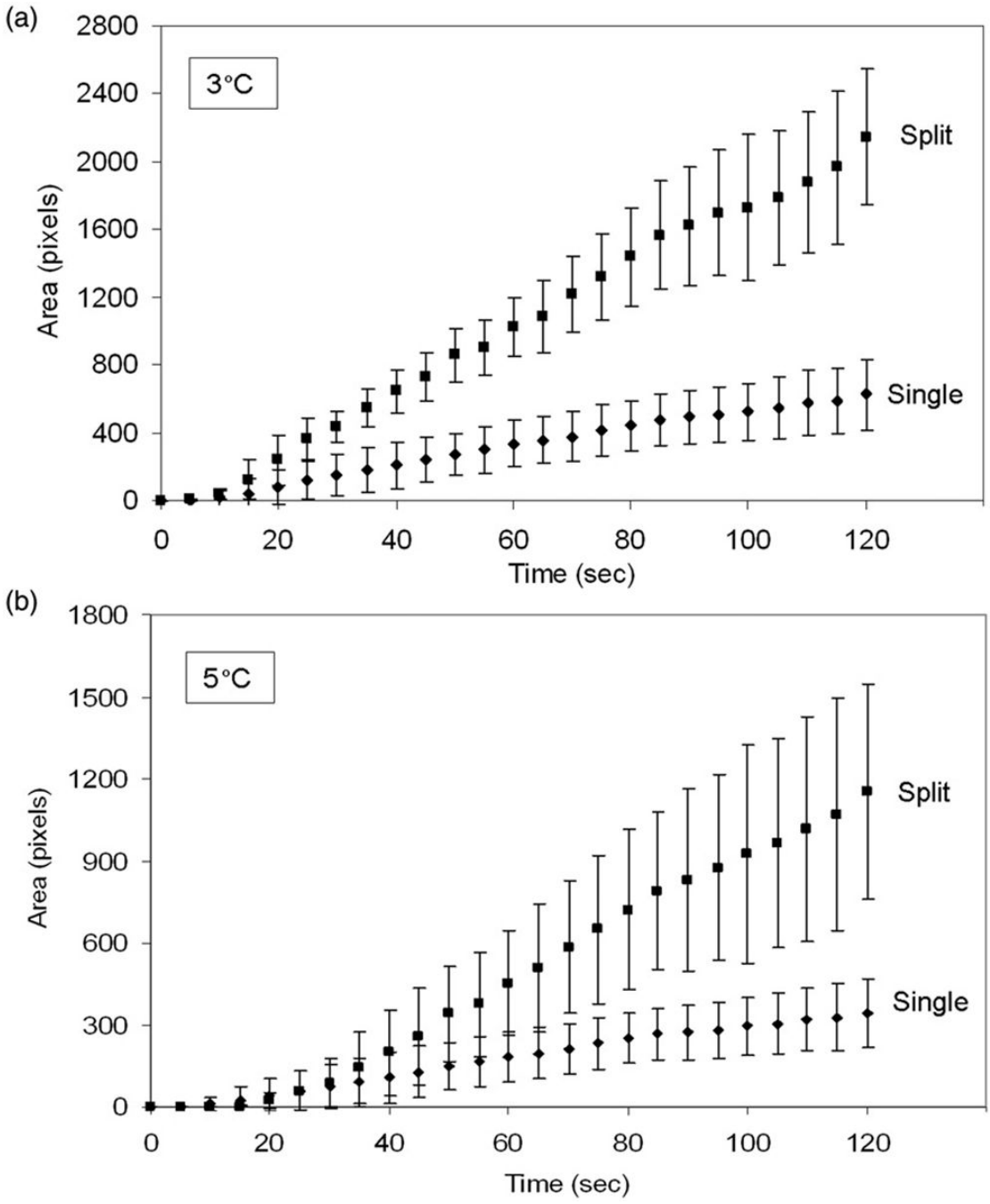

Figure 4.
Spatial temperature elevation greater than 3°C and 5°C during HIFU exposure with single focus and split focus transducers. Points, mean (n = 7); bars, standard deviation.

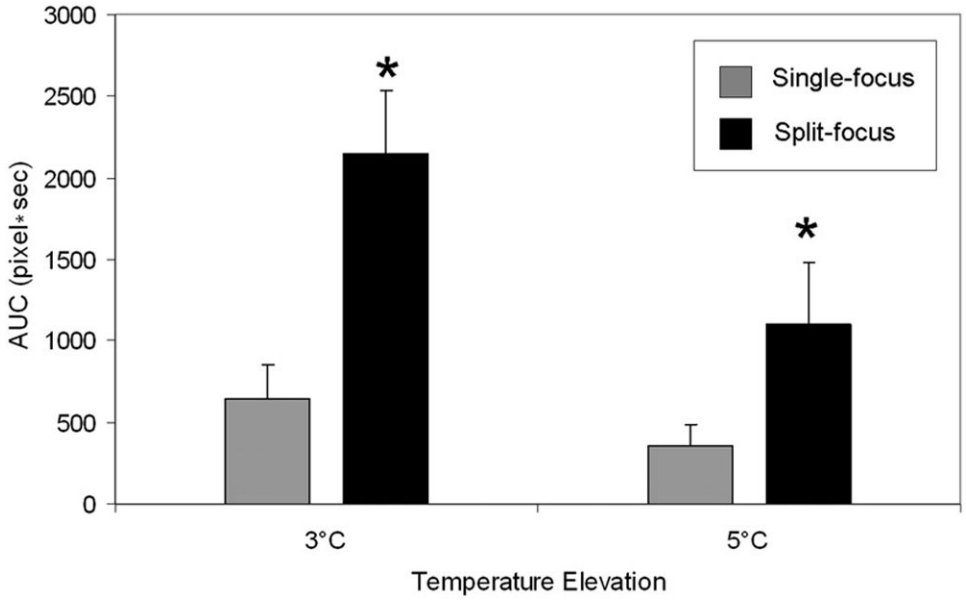

Figure 5.
Area under the curve for spatial temperature elevation greater than 3°C and 5°C during HIFU exposure with single focus and split focus transducers. Columns, mean (n = 7); bars, standard deviation.

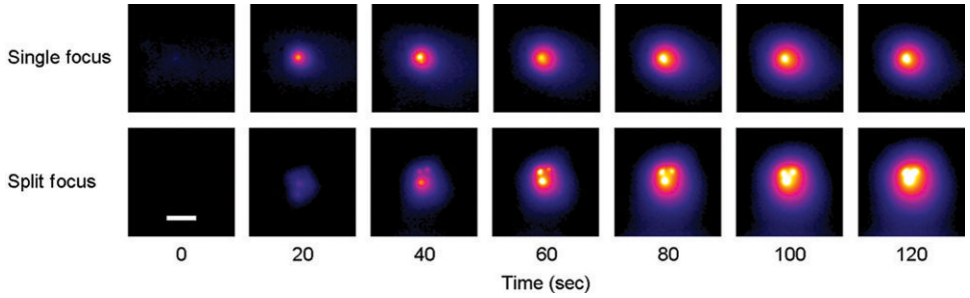

Figure 6.

Representative IR heating images for treatment of planar phantoms with single focus and split focus transducers, for a 120s exposure with each device. Images at early time points for the split focus device allow individual foci to be observed, which eventually meld together into a single larger focal spot (compared to the single focus device) by the end of the exposure. (Scale bar = 1 cm).

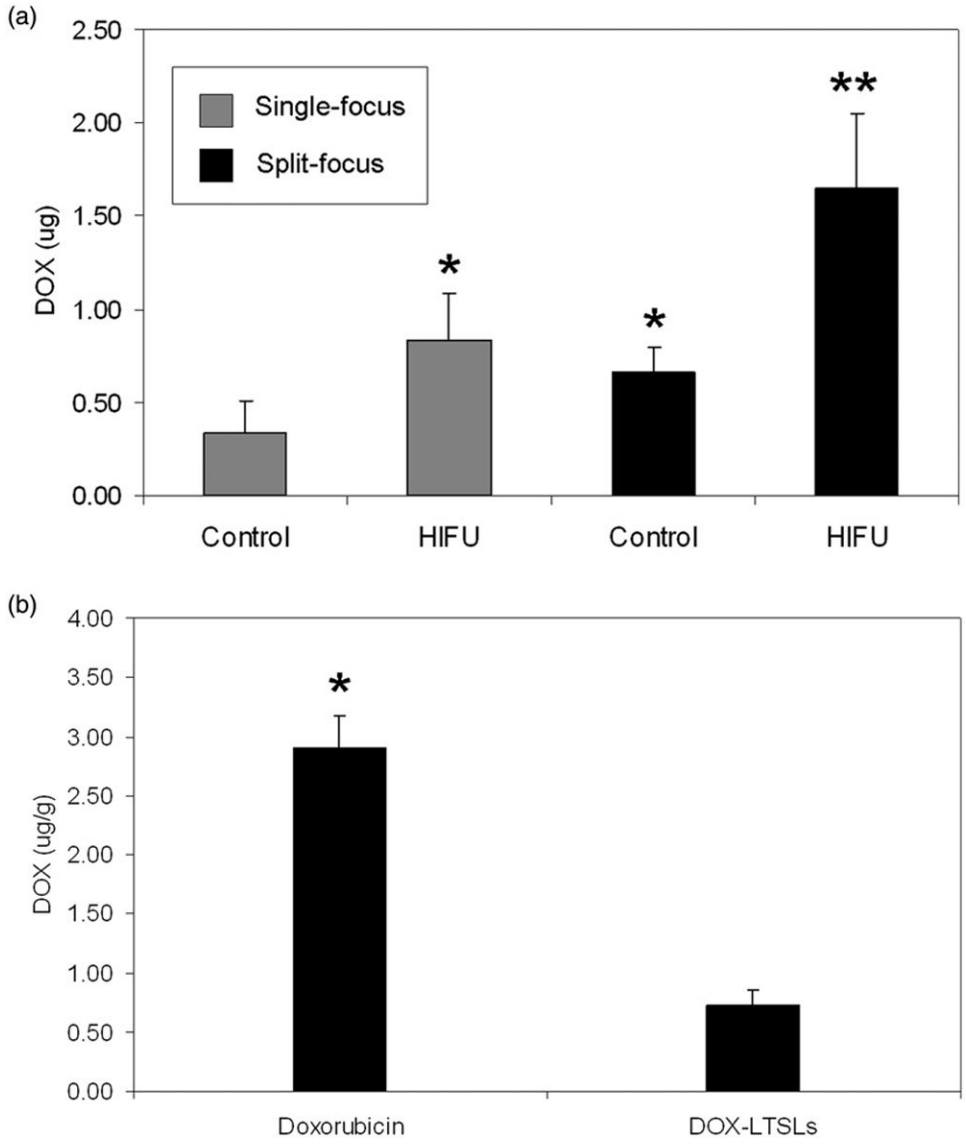

Figure 7.

(a) Total doxorubicin extracted from muscle in HIFU exposed extremity and control (unexposed) extremity for single focus and split focus transducers. (b) Concentration of doxorubicin found in muscle following treatment with free doxorubicin and LTSL-doxorubicin. No HIFU exposure. Columns, mean (n = 5); bars, standard deviation.

Table I

Experimental exposures.

		Exposed object	Transducer	Power (W)	Duty cycle (%)	*n*
I	1	Cylindrical phantom	Single focus	20	10	3
	2	Cylindrical phantom	Single focus	80	10	5
	3	Cylindrical phantom	Single focus	80	20	5
	4	Cylindrical phantom	Single focus	80	30	5
	5	Cylindrical phantom	Single focus	80	40	5
	6	Mouse tumor	Single focus	20	10	5
II	7	Planar phantom	Single focus	20	50	7
	8	Planar phantom	Split focus	30	50	7
	9	Planar phantom	Split focus	40	50	7
	10	Planar phantom	Split focus	50	50	7
	11	Planar phantom	Split focus	80	50	7
III	12	Mouse muscle[a]	Single focus	20	10	5
	13	Mouse muscle[a]	Split focus	80	10	5
	14	Mouse muscle[a]	n/a	n/a	n/a	5
	15	Mouse muscle[b]	n/a	n/a	n/a	5

All exposures were given at 1 MHz, pulse repetition frequency of 1 Hz, and 120 pulses per exposure.

[a] Low temperature sensitive liposomes;

[b] free doxorubicin.

Table II

Single to split focus comparisons.

	X-intercept	Slope	R^2	AUC*	Fold increase
3°C increase					
Single focus	2.34	5.47	0.9941	37891	1.0
Split focus	4.97	18.44	0.9957	121979	3.2 (P<0.001)
5°C increase					
Single focus	3.89	3.09	0.9935	20814	1.0
Split focus	14.69	10.62	0.9804	58880	2.8 (P<0.002)

*AUC, area under the curve as determined by integrating the equation describing the linear relationship between area increase and time.